ISSN 0389-4010
UDC 533.6.697, 536.7.75
621.454, 629.7.036.5

TECHNICAL REPORT OF NATIONAL AEROSPACE LABORATORY

TR-1199T

EFFECT OF REGENERATIVE COOLING ON ROCKET ENGINE SPECIFIC IMPULSE

Takeshi Kanda, Goro Masuya, Yoshio Wakamatsu
Akio Kanmuri, Nobuo Chinzei and Masayuki Niino

April 1993

NATIONAL AEROSPACE LABORATORY

CHOFU, TOKYO, JAPAN

EFFECT OF REGENERATIVE COOLING ON ROCKET ENGINE SPECIFIC IMPULSE*

Takeshi Kanda*1 Goro Masuya*1 Yoshio Wakamatsu*1
Akio Kanmuri*1 Nobuo Chinzei*1 and Masayuki Niino*1

ABSTRACT

The effects and limitations of regenerative cooling on rocket engine specific impulse was investigated with a quasi one-dimensional simulation model. Regenerative cooling of a rocket engine nozzle skirt was shown to increase engine specific impulse, and such increase being explained in two ways: net entropy depression in the engine, and acceleration of the supersonic heated gas by cooling. When the Reynolds number of the combustion gas was small, the regenerative cooling effect on specific impulse became relatively large.

Keywords: Liquid rocket engine, Regenerative cooling, Specific impulse, Entropy, Supersonic flow

概　　要

再生冷却が液体ロケットエンジンの比推力に及ぼす効果について，準一次元シミュレーションモデルを用いて検討した。ロケットエンジンのノズルスカートの再生冷却は，エンジン比推力を向上させることがわかった。この効果について，(1)エンジン全体のエントロピー増加の抑制，(2)加熱された超音速燃焼ガスを冷却することによる加速，というふた通りの説明を行った。また，レイノルズ数が小さい場合のほうが，再生冷却の効果が顕著であることを示した。この再生冷却の効果の限界についても議論を行なった。

Nomenclature

A =cross section
b =constant in the Blasius formula
B =constant in the Blasius formula
C.C. =combustion chamber
c_f =friction coefficient
Cp =specific heat at constant pressure
d =diameter
D_f =friction drag
F =impulse function
h =heat transfer coefficient, enthalpy
HO =total enthalpy
ΔHO =total enthalpy increment
Isp =specific impulse
M =Mach number
$\dot{m}$ =mass flow rate
N.S. =nozzle skirt
P =static pressure
PO =total pressure
Q =heat
ΔQ =heat increment
R =gas constant
Re =Reynolds number
R.C. =regenerative cooling
s =surface area
ΔS =entropy increment
Tw =wall temperature
TO =total temperature
u =velocity
x =distance
y =mole fraction
γ =specific heat ratio
μ =viscosity
ρ =density

* received 22. February 1993
*1 Kakuda Research Center

Subscripts

c =combustion
CC =combustion chamber
ex =regenerative heat exchange
H =hydrogen
m =mean
mix =mixing
NS =nozzle skirt
O =oxygen
ref =reference condition
th =throat
v =vacuum
1,1′ =entrance, reactor
2 =exit, product

1. Introduction

Regenerative cooling is a well-known engine cooling method, first conceived in 1942.[1] It is presently used in many rocket engines, e.g., the Space Shuttle main engine (SSME), and LE-7,[2] the booster engine of the Japanese rocket vehicle, H-II. In regenerative cooling, propellant is used as engine coolant, and the heated coolant is injected into a combustion chamber. This mechanism is called enthalpy pumping.[3] Regenerative cooling does not necessitate excess propellant to cool an engine, in contrast with other cooling methods such as film cooling, and dump cooling.

In the beginning of the liquid rocket engine study, several basic suggestive thermodynamical investigations were carried out.[4-6] It was described in Ref.5 that the regenerative cooling increases specific impulse due to entropy decrement of the combustion gas in the nozzle skirt. The investigation was, however, only on the combustion gas flow, and did not take entropy increment of coolant into consideration as a part of a whole engine. Engine cycle performance is specified by the net entropy increment in an engine: the smaller the net entropy increment, the better the engine performance in the Mollier diagram. The relation between engine performance and entropy increment must be discussed in a whole engine system. When a part of the whole engine is picked up, the entropy may decrease in it. For example, in a water-cooled nozzle skirt, entropy decreases because of cooling, i.e., because of extraction of energy. And there were not sufficient discussion on the difference of entropy increment in a subsonic flow and in a supersonic flow in the references.

In this report, to investigate the effect of regenerative cooling on rocket engine specific impulse, a whole liquid rocket engine was studied with a quasi one-dimensional simulation model, taking entropy increment of coolant into consideration.

2. Simulation

2.1 Model engine

Fig. 1 is a schematic of the model engine used. Pro-

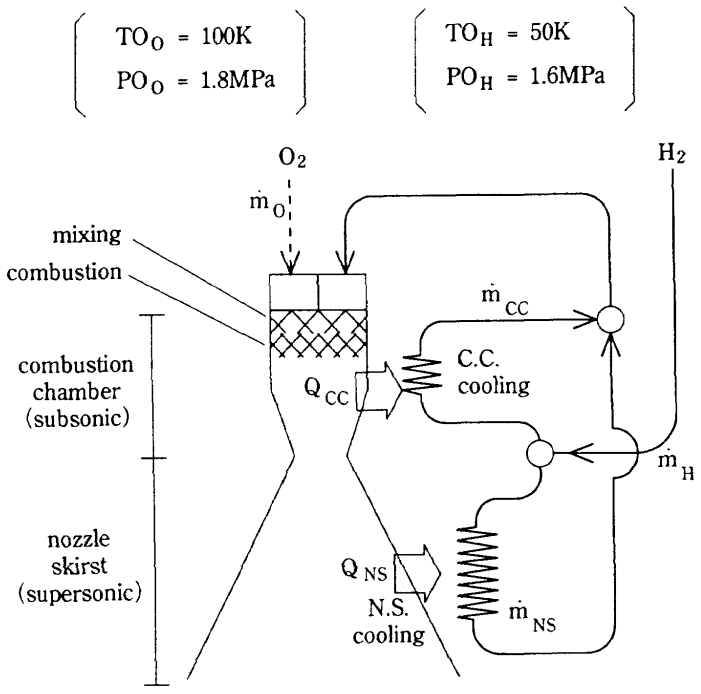

Fig. 1 Engine schematic

pellants were hydrogen and oxygen, and the hydrogen was also used to cool the combustion chamber and the nozzle skirt. In this report, an engine with regenerative cooling only at the nozzle skirt is termed a "N.S. cooled" engine, while an engine with regenerative cooling only at the combustion chamber is termed a "C.C. cooled" engine. An engine without regenerative cooling is termed a "no R.C." engine. In the "N.S. cooled" engine, hydrogen flowed only at the nozzle skirt cooling jacket, while in the "C.C. cooled" engine, it flowed only at the combustion chamber cooling jacket. In the model engine, the hydrogen flow rate was 40 $kg \cdot s^{-1}$ and the mixture ratio was O/F=6. The hydrogen properties were specified upstream of the regenerative cooling jacket, while the oxygen properties were specified upstream of the injector. The combustion chamber diameter was 0.4m, and the length was 0.4m. The nozzle skirt was conical with a length of 2.5m, and the nozzle expansion area ratio was 60. There were 288 cooling tubes around the combustion chamber, and there were 721 such tubes around the nozzle skirt. Mean height of the cooling tubes was 10mm, mean width of the tubes around the combustion chamber was 2mm, and mean width of the tubes around the nozzle was 10mm. The engine was as large as the LE-7.[2]

2.2 Assumptions and simulation methods

Fluids in the engine were compressible, calorically perfect gases. Gas species were hydrogen, oxygen, and a combustion product of water and hydrogen. Enthalpy of each gas was 0 at 0 K. Viscosity of the combustion product was calculated as a mixture of hydrogen and water.[7]

The gas flow was quasi one-dimensional. Basic equations were as follows, and they were used for the combustion gas flow as well as for the coolant flow.

$$\rho_2 u_2 A_2 = \rho_1 u_1 A_1 \tag{1}$$

$$(\rho_2 u_2^2 A_2 + P_2 A_2) - (\rho_1 u_1^2 A_1 + P_1 A_1) = P_m(A_2 - A_1) - F \tag{2}$$

$$\left(\frac{\gamma}{\gamma-1} P_2 u_2 A_2 + \frac{1}{2}\rho_2 u_2^3 A_2\right) - \left(\frac{\gamma}{\gamma-1} P_1 u_1 A_1 + \frac{1}{2}\rho_1 u_1^3 A_1\right) = Q \tag{3}$$

$$P_m(A_2 - A_1) = \int_1^2 P dA$$

Properties, e.g., density, velocity, pressure, entropy, etc., of the downstream portion were obtained as solutions of the above simultaneous quadratic equations. When two parallel flows joined and mixed, and became one flow, other upstream terms were added to the equations as shown in Eqs. (1') – (3').

$$\rho_2 u_2 A_2 = \rho_1 u_1 A_1 + \rho_1' u_1' A_1' \tag{1'}$$

$$(\rho_2 u_2^2 A_2 + P_2 A_2) = (\rho_1 u_1^2 A_1 + P_1 A_1) + (\rho_1' u_1'^2 A_1' + P_1' A_1') \tag{2'}$$

$$\left(\frac{\gamma}{\gamma-1} P_2 u_2 A_2 + \frac{1}{2}\rho_2 u_2^3 A_2\right) = \left(\frac{\gamma}{\gamma-1} P_1 u_1 A_1 + \frac{1}{2}\rho_1 u_1^3 A_1\right) + \left(\frac{\gamma}{\gamma-1} P_1' u_1' A_1' + \frac{1}{2}\rho_1' u_1'^3 A_1'\right) \tag{3'}$$

In this case, there was not heat addition, nor external force. The sum of the cross sections of the two upstream flows, $A_1 + A_1'$, was the same with the cross section of the downstream flow, A_2.

For example, the entropy increment due to the mixing at a constant cross section component was expressed with as follows, using the obtained properties of the downstream portion.

$$\Delta S_{mix} = \frac{\dot{m}_1}{\dot{m}_1 + \dot{m}_1'} \Delta S_{1\to 2} + \frac{\dot{m}_1'}{\dot{m}_1 + \dot{m}_1'} \Delta S_{1'\to 2} \tag{4}$$

$$\Delta S_{1\to 2} = -CP_1 \ln\left\{\dot{m}_1\sqrt{\gamma R_1 TO_1}\,\frac{M_1 + \frac{1}{\gamma M_1}}{\sqrt{1+\frac{\gamma-1}{2}M_1^2}} + \dot{m}_1'\sqrt{\gamma R_1' TO_1'}\,\frac{M_1' + \frac{1}{\gamma M_1'}}{\sqrt{1+\frac{\gamma-1}{2}M_1'^2}} \pm \sqrt{\beta}\right\}$$

$$+ Cv_1 \ln\left\{\dot{m}_1\sqrt{\gamma R_1 TO_1}\,\frac{M_1 + \frac{1}{\gamma M_1}}{\sqrt{1+\frac{\gamma-1}{2}M_1^2}} + \dot{m}_1'\sqrt{\gamma R_1' TO_1'}\,\frac{M_1' + \frac{1}{\gamma M_1'}}{\sqrt{1+\frac{\gamma-1}{2}M_1'^2}} \pm \gamma\sqrt{\beta}\right\}$$

$$+ R_1 \ln\left\{\frac{\dot{m}_1}{PO_1}\sqrt{\gamma R_1 TO_1}\,\frac{(1+\frac{\gamma-1}{2}M_1^2)^{\frac{\gamma+1}{2(\gamma-1)}}}{\gamma M_1} + \frac{\dot{m}_1'}{PO_1'}\sqrt{\gamma R_1' TO_1'}\,\frac{(1+\frac{\gamma-1}{2}M_1'^2)^{\frac{\gamma+1}{2(\gamma-1)}}}{\gamma M_1'}\right\}$$

$$+Cp_1\ln\left\{\frac{\gamma}{\gamma-1}R_1TO_1\dot{m}_1+\frac{\gamma}{\gamma-1}R_1'TO_1'\dot{m}_1'\right\}+Cv_1\ln\frac{\rho_1^{\gamma}}{P_1}-Cp_1\ln(\dot{m}_1+\dot{m}_1')-R_1\ln y_1$$

$$-Cp_1\ln\frac{R_{mix}}{R_1}+Cp_1\ln\frac{2(\gamma-1)}{\gamma}-Cv_1(\gamma+1)$$

$$\beta=\left(\dot{m}_1\sqrt{\gamma R_1TO_1}\frac{M_1+\frac{1}{\gamma M_1}}{1+\frac{\gamma-1}{2}M_1^2}+\dot{m}_1'\sqrt{\gamma R_1'TO_1'}\frac{M_1'+\frac{1}{\gamma M_1'}}{\sqrt{1+\frac{\gamma-1}{2}M_1'^2}}\right)^2-2\frac{(\gamma^2-1)}{\gamma^2}(\dot{m}_1+\dot{m}_1')\left(\frac{\gamma}{\gamma-1}R_1TO_1\dot{m}_1+\frac{\gamma}{\gamma-1}R_1'TO_1'\dot{m}_1'\right)$$

There was a mole fraction term of the fluid of 1, y_1, in the ΔS_{1-2} term due to the change of partial pressure. Ratio of specific heats was not distinguished in the expression because both hydrogen and oxygen are molecules with two atoms, and their ratios are not so different each other. They were set to 1.4 in this investigation. One of the complex sign in front of the square root of β in the ΔS_{1-2} term had a meaning physically. It depended on the conditions of the two flows before the mixing. For example, when both flows were supersonic, the sign was a minus. The $\Delta S_{1'-2}$ term was expressed similar to the ΔS_{1-2} term.

The entropy increment due to heating/cooling at a constant cross section component was expressed as follows. One of the complex sign in front of the square root of α had a meaning physically, being similar to the complex sign of the mixing shown in Eq. (4).

$$\Delta S=-Cp\ln\left\{\frac{1+\gamma M_1^2-\frac{D_t}{A_1PO_1}\left(1+\frac{\gamma-1}{2}M_1^2\right)^{\frac{\gamma}{\gamma-1}}\pm\sqrt{\alpha}}{2\left(1+\frac{\gamma-1}{2}M_1^2\right)\left(1+\frac{Q}{\dot{m}CpTO_1}\right)}\right\}+Cv\ln\left\{\frac{1}{\gamma+1}\left\{1+\gamma M_1^2-\frac{D_t}{A_1PO_1}\left(1+\frac{\gamma-1}{2}M_1^2\right)^{\frac{\gamma}{\gamma-1}}\pm\gamma\sqrt{\alpha}\right\}\right\} \quad (5)$$

$$\alpha=\left\{1+\gamma M_1^2-\frac{D_t}{A_1PO_1}\left(1+\frac{\gamma-1}{2}M_1^2\right)^{\frac{\gamma}{\gamma-1}}\right\}^2-2(\gamma+1)M_1^2\left(1+\frac{\gamma-1}{2}M_1^2\right)\left(1+\frac{Q}{\dot{m}CpTO_1}\right)$$

Injected hydrogen and oxygen were fully mixed. The mixture fully reacted. There was no dissociation. There was no total pressure loss in bends, nor in manifolds.

There were two kinds of simulation in this report.

Simulation A

In Simulation A, regeneratively exchanged heat was a parameter. The exchanged heat was specified, and the heat was distributed uniformly along the gas flow before starting simulation calculation. The combustion gas was inviscid. And the heat exchage was carried out at the part of the constant cross section, as mentioned below. So the combustion gas flow was the Rayleigh flow in Simulation A.

Simulation B

In Simulation B, more realistic simulation was carried out, i.e., regenerative heat exchange was calculated assuming a uniform temperature engine wall and viscous combustion gas. The wall temperature was calculated to balance the total heat flux from the combustion gas and that to the coolant. The heat transfer coefficient and the friction coefficient in the combustion chamber and in the nozzle skirt were calculated with the Blasius formula and Reynolds analogy.[8] Reynolds number of the "no R.C." engine at the throat was 13×10^6.

In both kinds of simulation, to simulate flow in a convergent/divergent part of the engine, convergent/divergent parts of the combustion chamber and of the nozzle skirt were divided into a hundred sections respectively. Each section was divided into two parts, i.e.,

(1) The divergent part where the combustion gas expanded isentropically.

(2) The constant cross section part where heat exchage occurred.

The entropy increment due to chemical reaction was calculated with standard entropy of each species.

$$\Delta S_c=S_2-S_1 \quad (6)$$

$$S_1=\frac{1}{\sum_i\dot{m}_i}\sum_i\dot{m}_i\left\{Cp_i\ln(T_{i,1}-T_{i,0})-R_i\ln P_{i,1}+S_{i,0}\right\}$$

The S_2 term was expressed similar to the S_1 term in Eq. (6).

In both kinds of simulation, hydrogen was viscous in the cooling tubes. The friction coefficient was calcu-

lated with the universal resistance law for smooth pipes,[9] and Reynolds analogy was used to calculate the heat transfer coefficient. The equations for friction drag and heat flux are as follows:

$$D_f = \int \frac{c_f \rho u^2}{2} ds$$

$$= \int \frac{2\dot{m} c_f u}{d} dx \quad (7)$$

$$Q_{ex} = \int h(T_r - T_w) ds$$

$$= \int \frac{2\dot{m} c_f Cp(T_r - T_w)}{d} dx \quad (8)$$

For heat transfer from the combustion gas, Eq.(8) can also be expressed as follows.

$$Q_{ex}/Q_c = \int \frac{2\, c_{f,c}\, Cp_c\, (TO_c - Tw_c)}{d_c\, \Delta HO_c} dx \quad (9)$$

Q_c is combustion heat release, $\dot{m}$ is propellant flow rate, and the enthalpy increment, ΔHO_c, is as follows:

$$Q_c = \dot{m}\, \Delta HO_c \quad (10)$$

For Blasius formula,

$$c_f = 2B\, Re_x^{-b} \quad (11)$$

Eqs.(7) and (8) can be expressed as follows with mean values.

$$D_f = B \frac{\rho^{1-b} u^{2-b} \mu^b s}{2x^b} \quad (12)$$

$$Q_{ex} = B \frac{\rho^{1-b} u^{1-b} \mu^b s\, Cp(T_r - T_w)}{x^b} \quad (13)$$

In the above equations, b=0.2, and B=0.0296 for turbulent flow.

2.3 Simulation results

The effect of regenerative cooling on engine specific impulse in Simulation A is shown in Fig. 2 with solid lines. The regeneratively exchanged heat is non-dimensionalized with the combustion heat release. Total temperature of hydrogen after regenerative cooling is also shown. When the nozzle skirt was cooled regeneratively, the specific impulse increased with the exchanged heat ("N.S. cooling" in Fig. 2). When the combustion chamber was cooled, however, the specific impulse did not increase, but was the same as that of the "no R.C." engine ("C.C. cooling" in Fig. 2). In Fig. 2, specific impulses by Simulation B are indicated with circles. These impulses were smaller than those of Simulation A due to friction. The specific impulses of the "N.S. cooled" and the "N.S. & C.C. cooled" engines were 4390 $m \cdot s^{-1}$, while those of the "C.C. cooled" and the "no R.C." engines were 4375$m \cdot s^{-1}$. The engine specific impulse increased only when a nozzle skirt was cooled regeneratively. Regenerative cooling of the combustion chamber did not greatly affect the specific impulse. Pressures in the combustion chamber were around 15 MPa in all the simulations in Fig. 2.

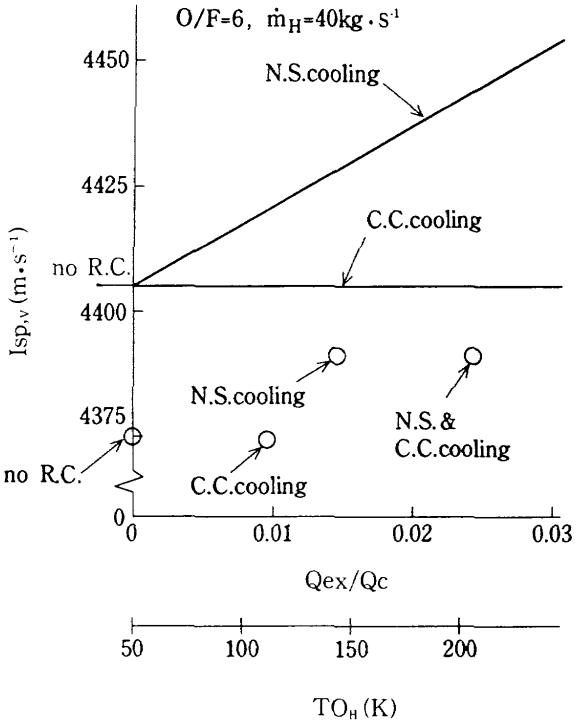

Fig. 2 The effect of regenerative cooling on specific impulse
Lines indicate results of frictionless simulation (Simulation A), and circles represent results of simulation with friction (Simulation B).

Fig. 3 shows specific impulse increment with nozzle expansion area ratio. Broken and solid lines represent results of Simulation A and those of B, respectively. There was a regenerative cooling effect on specific impulse in all expansion area ratios. In Simulation B, the effect increased with the expansion area ratio, because non-dimensional regeneratively exchanged heat increased from 1% at the expansion area ratio of 60 to 3% at 1000.

When a rocket engine is used in an orbital transfer vehicle, or in an aerospace-plane, it may often be throttled. Fig. 4 shows specific impulses of a reduced propellant flow rate operation. The propellant flow rate is non-dimensionalized with the reference propellant flow rate, i.e., the sum of hydrogen with a flow rate of 40

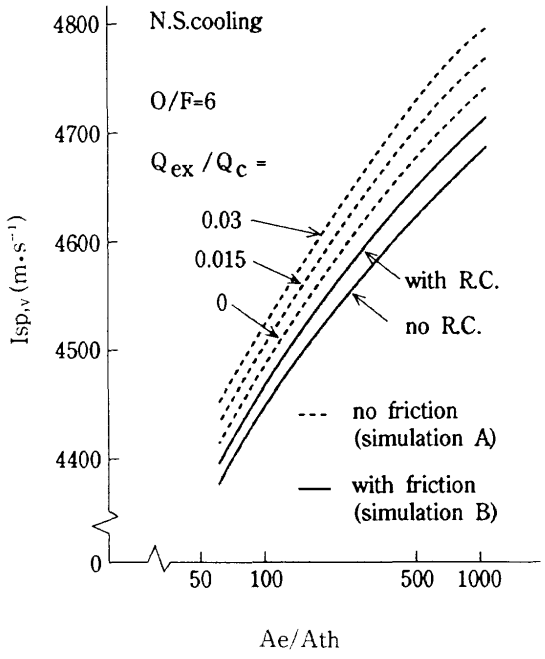

Fig. 3 The effect of regenerative cooling at various nozzle area ratios

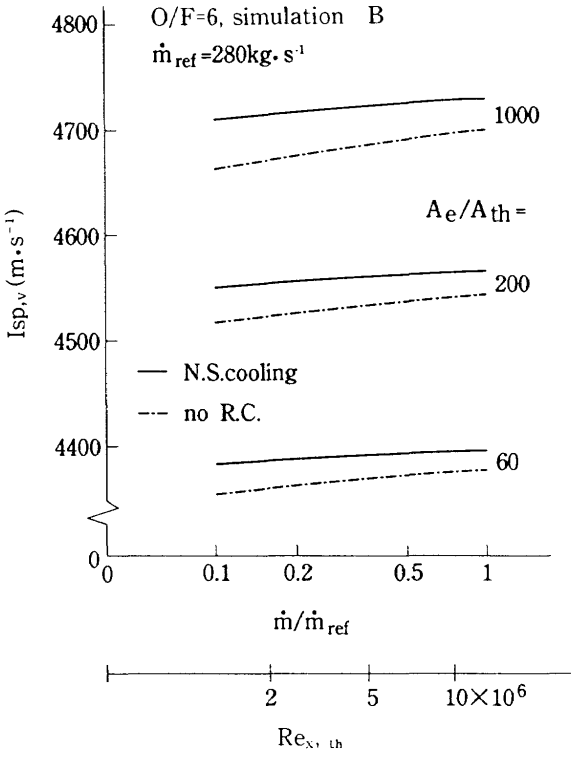

Fig. 4 The effect of throttling on specific impulse

kg·s^{-1} and oxygen with a flow rate of 240 kg·s^{-1}. The engine geometry was not changed. Propellant total pressures were reduced proportionally with the flow rate changes. Reynolds number of the "N.S. cooled" engine at the throat is also shown. The regenerative cooling effect on specific impulse became large when the propellant flow rate was reduced.

3 Discussion

There is no difference in flow conditions due to hydrogen heating, injection, and combustion processes between in the "N.S. cooled" engine and in the "C.C. cooled" engine with the same amount of heat exchange. The cause of the specific impulse increment lies in the cooling process of the combustion gas. It was discussed previously,[4] but the description was not enough to explain the mechanism of the effect of regenerative cooling on the specific impulse completely. The previous discussion was limited on the combustion gas, but the discussion did not pay enough attention to flow conditions, e.g., subsonic flow or supersonic flow.

We will explain it in two ways. The propellant flow rate reduction effect shown in Fig. 4 and the limit of the regenerative cooling effect are also discussed.

3.1 Entropy increment in the engine

Fig. 5 shows the net entropy increment in the "N.S. cooled" engine, and Fig. 6 shows that in the "C.C. cooled" engine. Due to regenerative cooling, entropy increment of combustion decreased very much because of the increment of total temperature of the mixed propellants. At around 0.01 of Q_{ex}/Q_c the entropy increment on mixing became smallest. Entropy increment of heating hydrogen increased with the regeneratively exchanged heat. Finally, the net entropy increment of "N.S. cooled" engine became small with the regeneratively exchanged heat. In contrast, the net entropy of the "C.C. cooled" engine did not change very much, even though the combustion chamber was regeneratively cooled.

Engine cycle performance is specified by the entropy increment in an engine: the smaller the entropy increment, the better the engine performance in the Mollier diagram. In Rayleigh flow, the higher the entrance Mach number, the larger the entropy decrease by cooling due to heat absorption.[10] This is expressed as a solution of Eqs. (1) – (3) with constant cross section and inviscid flow conditions as shown in Eq. (5) (Fig. 7). In the subsonic region, the entropy decrease is roughly con-

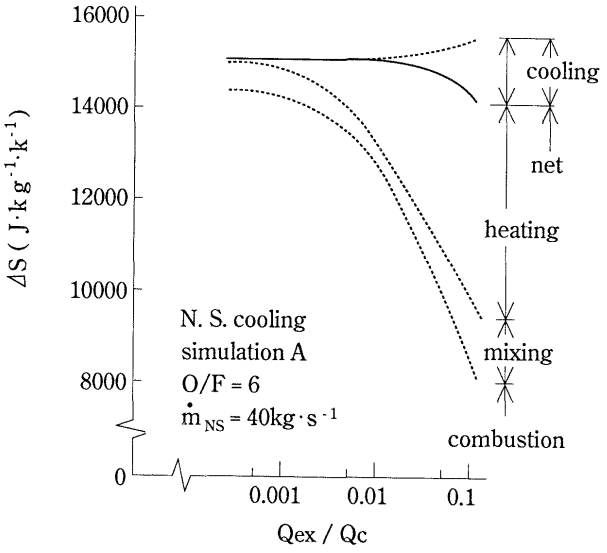

Fig. 5 Entropy change with regeneratively exchanged heat in "N. S. cooled" engine

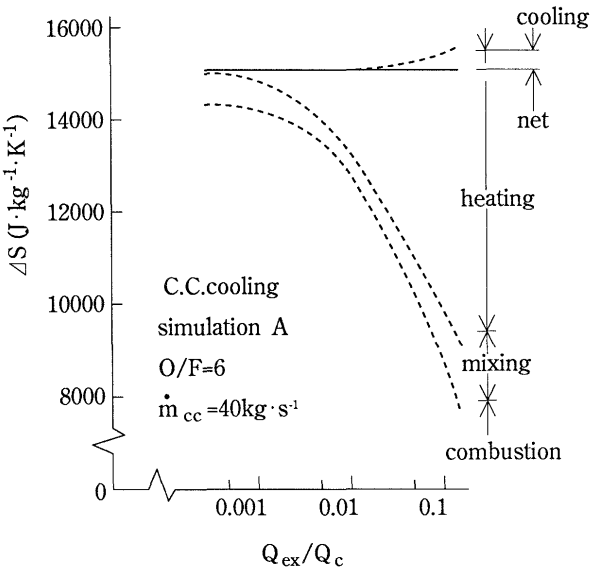

Fig. 6 Entropy change with regeneratively exchanged heat in "C. C. cooled" engine

stant.

In regenerative cooling, heat is transferred from the subsonic flow in the combustion chamber and from the supersonic flow in the nozzle skirt to the subsonic coolant flow. The net entropy increment in the engine becomes small, and the engine specific impulse becomes great when the supersonic gas is cooled in the nozzle skirt. There is no use to cool the subsonic combustion gas in the combustion chamber in order to increase specific impulse.

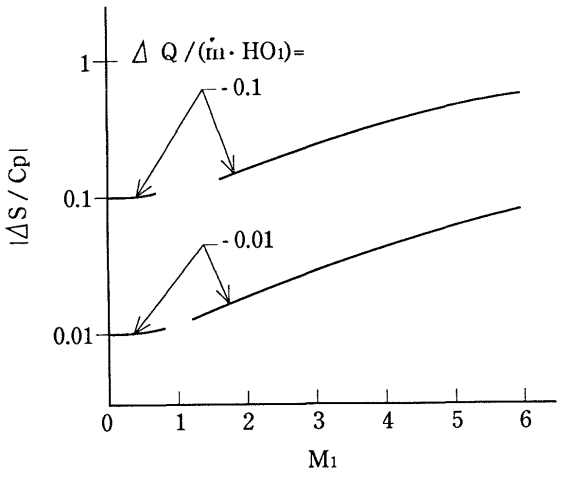

Fig. 7 Entropy-Mach number in cooling

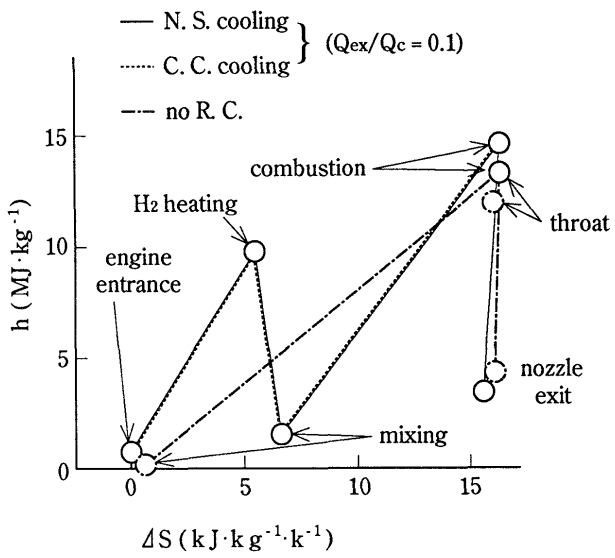

Fig. 8 Mollier diagram

Fig. 8 shows the comparison of the model engine operations by Simulation A in a Mollier diagram. The net entropy increment became smaller, the enthalpy at the cycle end point, which corresponded to the nozzle skirt exit, was lower, and the kinetic energy was greater in the "N.S. cooled" engine than in the other two engines, i.e., in the "no R.C." engine, and in the "C.C. cooled" engine.

3.2 Impulse function increment in engine

Engine vacuum thrust is equal to the impulse function at the nozzle exit. The impulse function can be written as follows.

$F = \dot{m}u + PA$

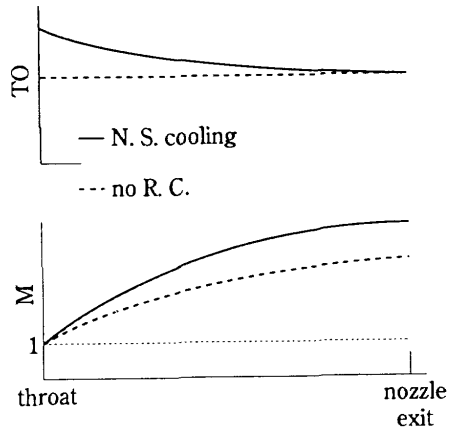

Fig. 9 Total temperature and Mach number in "N. S. cooled" engine nozzle

$$=\dot{m}\sqrt{\frac{RTO}{\gamma}}\ \frac{(1+\gamma M^2)}{M}\ \sqrt{1+\frac{(\gamma-1)}{2}M^2} \qquad (14)$$

It increases with Mach number in a supersonic region.

Total temperature at the exit of the regeneratively cooled engine is the same as that of the "no R.C." engine. However, in the "N.S. cooled" engine, the total temperature at the throat is higher than that of the "no R.C." engine because heat absorbed by the coolant hydrogen from the nozzle flow is fed to the combustion chamber. The combustion gas is accelerated not only by the divergence of the nozzle, but also by the cooling in the supersonic portion of the engine, i.e., in the nozzle skirt. Mach number and impulse function at the exit of the "N.S. cooled" engine become larger than those of the "no R.C." engine (Fig. 9).

In the "C.C. cooled" engine, no acceleration results from the regenerative cooling of the combustion chamber, and there is no increment of specific impulse due to the regenerative cooling of the combustion chamber.

3.3 Reynolds number effect

In this section, the effect of Reynolds number in the regenerative cooling effect is discussed using the results of the reduced propellant operation shown in Fig. 4. The velocity, the temperature, and thus the viscosity of the combustion gas do not change very much due to the propellant flow rate in the specified engine shape. Therefore, the Reynolds number in Eq. (11) is proportional to the propellant flow rate, and the friction coefficient is proportional to -0.2 power of the propellant flow rate.

The specific impulse increment is proportional to the regeneratively exchanged heat as seen in Fig. 2. According to Eq. (8), the total enthalpy increment due to regenerative cooling is proportional to the friction coefficient, so the specific impulse increment is proportional to the friction coefficient, and also proportional to the -0.2 power of the Reynolds number, e.g., the propellant flow rate.

As shown in Fig. 4, in a small Reynolds number range, e.g., in a small propellant flow rate range, friction drag became large, and the specific impulses decreased with reduction of the propellant flow rate. But due to the effect of the -0.2 power, the specific impulse of the "N.S. cooled" engine became relatively larger than that of the "no R.C." engine. This effect can be obtained with a change of other factors of Reynolds number, e.g., engine scale. Therefore, friction drag can be partially compensated for by regenerative cooling.

3.4 Limit of regenerative cooling effect on specific impulse

The regeneratively exchanged heat in Simulation B was estimated to be only 1~3% of the heat release of combustion, and it resulted in an engine specific impulse increase of 15~30m·s^{-1}, or 0.3~0.6% of the"no R.C." engine specific impulse. However, it would be difficult to increase the regenerative cooling effect drastically. According to Eqs. (7) and (8), the area where heat flux is large corresponds to the area where friction force is large. Therefore, it is not useful to enlarge the nozzle surface area, e.g., with fins, to obtain greater heat flux, and to increase the effect of regenerative cooling on specific impulse.

As seen in Fig. 3, the extended nozzle skirt increases specific impulse, but this is mainly due to the divergence of the nozzle, not to the increment of the regeneratively exchanged heat. Heat flux in the nozzle skirt becomes small downstream of the nozzle because of low density. Moreover, the friction force is proportional to the 1.8 power of velocity in Eq. (12), while the heat flux is proportional to the 0.8 power in Eq. (13). So it is not useful to extend the nozzle in order to enhance the regenerative cooling effect.

The effect of regenerative cooling on specific impulse generally seems to be an increment of ten or more meters per second at most. In other words, when regenerative cooling of the nozzle skirt is actively employed in a rocket engine, the specific impulse of the engine is

increased by ten or more meters per second.

4. Conclusions

The effect of regenerative cooling on specific impulse was investigated by simulation with short calculations, and its mechanism was discussed.

(1) When a supersonic component, i.e., a nozzle skirt, was cooled regeneratively, engine specific impulse became larger by ten meters or more per second than that of an uncooled engine. When a subsonic component, i.e., a combustion chamber, was cooled, however, specific impulse did not change.

(2) The effect was explained in two ways:
   (a) Great entropy reduction due to cooling of a supersonic flow in the nozzle skirt in comparison with little entropy reduction due to cooling of a subsonic flow in the combustion chamber.
   (b) Acceleration of the heated supersonic flow due to cooling in the nozzle skirt in comparison with no acceleration of the heated subsonic flow due to cooling in the combustion chamber.

(3) The effect became relatively large at small Reynolds numbers.

(4) Increasing the surface area in the nozzle skirt did not result in enhancement of the regenerative cooling effect. The increment of the specific impulse due to the effect was ten or more meters per second at most.

References

1) Stockel, K.; Zur Entwicklungsgeschichte des Hochdruch-Hauptstrom-Raketentriebwerks in Deutschland, Z. Flugwiss. Weltraumforsch, Vol.9, No.1 (1985/1-2) pp.1-14. (in German)

2) Kanmuri, A., Kanda, T., Wakamatsu, Y., Torii, Y., Kagawa, E., and Hasegawa, K.; Transient Analysis of LOX/LH2 Rocket Engine (LE-7), AIAA paper 89-2736 (1989/7).

3) Aerojet Liquid Rocket Co.; Orbit Transfer Vehicle (OTV) Advanced Expander Cycle Engine Point Design Study. Vol.II: Study Results, NASA CR-161638 (1980/12) pp.235.

4) Altman, D., Carter, J. M., and Penner, S.S.; Liquid Propellant Rockets (1960) pp.37-39, Princeton Univ. Press.

5) Banerian, G.; Rocket Performance with Heat Added to Inlet Propellants by Regenerative and External Means, Jet Propulsion, Vol.25, No.12 (1955) pp. 707-711.

6) Seifert, H., and Altman, D.; A Comparison of Adiabatic and Isothermal Expansion Processes in Rocket Nozzles, ARS Journal, Vol.22, No.3 (1952) pp.159-162.

7) Reid, R.C., Prausnitz, J. M., and Sherwood, T. K.; The Properties of Gases and Liquids (1977) pp.394-419, McGraw-Hill.

8) Mayer, E.; Analysis of Convective Heat Transfer in Rocket Nozzles, ARS Journal, Vol.31, No.7 (1961/7) pp.911-917.

9) Schlichting, H.; Boundary Layer Theory, (1979) McGraw-Hill, pp.610, McGraw-Hill.

10) Shapiro, A. H.; The Dynamics and Thermodynamics of Compressible Fluid Flow: Vol. I, (1953) pp.229-232, Ronald.

TECHNICAL REPORT OF NATIONAL
AEROSPACE LABORATORY
TR-1199T

航空宇宙技術研究所報告1199T号(欧文)

平成5年4月発行

発行所　航空宇宙技術研究所
東京都調布市深大寺東町7丁目44番地1
電話 三鷹(0422)47-5911(大代表)〒182
印刷所　株式会社　実業公報社
東京都千代田区九段北1-7-8

Published by
NATIONAL AEROSPACE LABORATORY
7-44-1 Jindaijihigashi-machi, Chōfu, Tokyo
JAPAN

Printed in Japan